A priori testing of subgrid-scale models for the velocity-pressure and vorticity-velocity formulations

By G. S. Winckelmans[1], T. S. Lund[2], D. Carati[3] AND A. A. Wray[4]

Subgrid-scale models for large eddy simulation (LES) in both the velocity-pressure and the vorticity-velocity formulations were evaluated and compared in *a priori* tests using spectral Direct Numerical Simulation (DNS) databases of isotropic turbulence: 128^3 DNS of forced turbulence ($Re_\lambda = 95.8$) filtered, using the sharp cutoff filter, to both 32^3 and 16^3 synthetic LES fields; 512^3 DNS of decaying turbulence ($Re_\lambda = 63.5$) filtered to both 64^3 and 32^3 LES fields. Gaussian and top-hat filters were also used with the 128^3 database. Different LES models were evaluated for each formulation: eddy-viscosity models, hyper eddy-viscosity models, mixed models, and scale-similarity models. Correlations between exact versus modeled subgrid-scale quantities were measured at three levels: tensor (traceless), vector (solenoidal 'force'), and scalar (dissipation) levels, and for both cases of uniform and variable coefficient(s). Different choices for the $1/T$ scaling appearing in the eddy-viscosity were also evaluated. It was found that the models for the vorticity-velocity formulation produce higher correlations with the filtered DNS data than their counterpart in the velocity-pressure formulation. It was also found that the hyper eddy-viscosity model performs better than the eddy viscosity model, in both formulations.

1. Velocity-pressure formulation and models investigated

Consider the Navier-Stokes equations for incompressible fluid in the velocity-pressure formulation:

$$\frac{\partial u_i}{\partial t} + \frac{\partial}{\partial x_j}(u_i u_j) + \frac{\partial P}{\partial x_i} = \nu \frac{\partial}{\partial x_j}\frac{\partial u_i}{\partial x_j} \; .$$

Filtering, using a low-pass filter G of characteristic length Δ,

$$\overline{\psi}(\boldsymbol{x}) = \int \psi(\boldsymbol{y})\, G\left(\frac{\boldsymbol{x}-\boldsymbol{y}}{\Delta}\right) \frac{d\boldsymbol{y}}{\Delta^3} \; , \qquad \psi'(\boldsymbol{x}) = \psi(\boldsymbol{x}) - \overline{\psi}(\boldsymbol{x}) \; ,$$

1 Dept. of Mechanical Engineering , Université catholique de Louvain, Belgium
2 Center for Turbulence Research
3 Dept. of Statistical Physics, Université libre de Bruxelles, Belgium
4 NASA Ames Research Center

with $\overline{\psi}$ the filtered value and ψ' the remainder, leads to the following evolution equation for the filtered velocity field:

$$\frac{\partial \overline{u}_i}{\partial t} + \frac{\partial}{\partial x_j}\left(\overline{u_i u_j}\right) + \frac{\partial \overline{P}}{\partial x_i} = \nu \frac{\partial}{\partial x_j}\frac{\partial \overline{u}_i}{\partial x_j} \ .$$

which is rewritten either as

$$\frac{\partial \overline{u}_i}{\partial t} + \frac{\partial}{\partial x_j}\left(\overline{u}_i \overline{u}_j\right) + \frac{\partial \overline{P}}{\partial x_i} + \frac{\partial \tau_{ij}}{\partial x_j} = \nu \frac{\partial}{\partial x_j}\frac{\partial \overline{u}_i}{\partial x_j} \ ,$$

or as

$$\frac{\partial \overline{u}_i}{\partial t} + \frac{\partial}{\partial x_j}\left(\overline{\overline{u}_i \overline{u}_j}\right) + \frac{\partial \overline{P}}{\partial x_i} + \frac{\partial \overline{\tau}_{ij}}{\partial x_j} = \nu \frac{\partial}{\partial x_j}\frac{\partial \overline{u}_i}{\partial x_j} \ .$$

where the 'subgrid-scale stress' (sgs) tensor is defined as

$$\tau_{ij} \stackrel{\text{def}}{=} \overline{u_i u_j} - \overline{u}_i \overline{u}_j = \overline{C}_{ij} + \overline{R}_{ij} + L'_{ij} \ ,$$
$$\overline{\tau}_{ij} \stackrel{\text{def}}{=} \overline{u_i u_j} - \overline{\overline{u}_i \overline{u}_j} = \overline{C}_{ij} + \overline{R}_{ij} \ ,$$

with the usual definitions for the cross term, the Reynolds term, and the Leonard's term:

$$\overline{C}_{ij} = \overline{\overline{u}_i u'_j} + \overline{u'_i \overline{u}_j} \ ,$$
$$\overline{R}_{ij} = \overline{u'_i u'_j} \ ,$$
$$L'_{ij} = \overline{\overline{u}_i \overline{u}_j} - \overline{u}_i \overline{u}_j = -\left(\overline{u}_i \overline{u}_j\right)' \ .$$

Here, $\overline{C}_{ij}$ and $\overline{R}_{ij}$ are purposely written with the 'overline' as they are the filtered value of some quantity. L'_{ij} is purposely written with the 'prime' as it is the remainder, after filtering, of some quantity and thus contains high spatial frequencies.

The notation $\overline{\tau}_{ij}$ is somewhat misleading (but will nevertheless be retained). Indeed, although it is the filtered value of some quantity, it is not necessarily the result of filtering τ_{ij}. In the case of sharp cutoff filter in wave space, $\overline{\overline{\psi}} = \overline{\psi}$ and $\overline{\psi'} = 0$ so that $\overline{\tau}_{ij}$ is indeed the result of filtering τ_{ij}. In the case of smooth filters such as the Gaussian, the filtering of τ_{ij} produces $\overline{\overline{C}}_{ij} + \overline{\overline{R}}_{ij} + \overline{L'}_{ij}$, which is not equal to $\overline{C}_{ij} + \overline{R}_{ij}$.

When doing LES with a computational grid which is of the same size as the assumed filter size Δ, one cannot accurately evaluate quadratic terms such as $(\overline{u}_i \overline{u}_j)$ using the coarse grid only, as such quantities have a high frequency content. One can only hope to resolve, on the coarse grid, quantities such as $\left(\overline{\overline{u}_i \overline{u}_j}\right)$ (and even that requires using an appropriate reconstruction scheme, e.g., the need for dealiasing in spectral codes). The second form of the filtered equation is thus the one to consider in LES computations. It is assumed throughout this paper unless otherwise specified. (Notice that, if one were to use a computational grid smaller than the assumed filter size, then quantities such as $\overline{u}_i \overline{u}_j$ could be partially resolved.)

The trace of the subgrid-scale tensor does not influence the dynamics of the filtered flow and is usually lumped into the pressure term:

$$\overline{\tau}^*_{ij} = \overline{\tau}_{ij} - \frac{1}{3}\overline{\tau}_{kk}\,\delta_{ij}\ , \qquad \overline{P}^* = \overline{P} + \frac{1}{3}\overline{\tau}_{kk}\ ,$$
$$\frac{\partial \overline{u}_i}{\partial t} + \frac{\partial}{\partial x_j}\left(\overline{\overline{u}_i\overline{u}_j}\right) + \frac{\partial \overline{P}^*}{\partial x_i} + \frac{\partial \overline{\tau}^*_{ij}}{\partial x_j} = \nu\frac{\partial}{\partial x_j}\frac{\partial \overline{u}_i}{\partial x_j}\ .$$

Only the subgrid scale force, the divergence of the subgrid-scale tensor $\overline{f}^*_i = \frac{\partial \overline{\tau}^*_{ij}}{\partial x_j}$, needs to be modeled: 3 degrees of freedom instead of 5, (or 6 if one were also interested in modeling $\overline{\tau}_{kk}$). The modified pressure is solution of

$$-\frac{\partial}{\partial x_i}\frac{\partial \overline{P}^*}{\partial x_i} = \frac{\partial}{\partial x_i}\frac{\partial}{\partial x_j}\left(\overline{\overline{u}_i\overline{u}_j}\right) + \frac{\partial \overline{f}^*_i}{\partial x_i}\ .$$

Finally, the solenoidal (i.e., divergence-free) part of the subgrid-scale force is the only one that affects the flow dynamics. Defining $\overline{g}^*_i$ as the solenoidal part of $\overline{f}^*_i$, the other part being the gradient of a potential $\overline{\phi}$ which is lumped into a new 'pressure', $\overline{\mathcal{P}}^* = \overline{P}^* + \overline{\phi}$, we write:

$$\frac{\partial \overline{u}_i}{\partial t} + \frac{\partial}{\partial x_j}\left(\overline{\overline{u}_i\overline{u}_j}\right) + \frac{\partial \overline{\mathcal{P}}^*}{\partial x_i} + \overline{g}^*_i = \nu\frac{\partial}{\partial x_j}\frac{\partial \overline{u}_i}{\partial x_j}\ ,$$
$$-\frac{\partial}{\partial x_i}\frac{\partial \overline{\mathcal{P}}^*}{\partial x_i} = \frac{\partial}{\partial x_i}\frac{\partial}{\partial x_j}\left(\overline{\overline{u}_i\overline{u}_j}\right)\ .$$

Correlations of different LES models with filtered DNS data in isotropic turbulence were obtained and investigated. This was done at three levels: tensor level (traceless sgs tensor), vector level (solenoidal force), and scalar level (dissipation), for two different DNS data sets, using the sharp cutoff filter in wave space (with spherical truncation):

a) 128^3 DNS of forced isotropic turbulence ($\mathrm{Re}_\lambda = 95.8$) that was filtered to both 32^3 and 16^3 synthetic LES fields, see Fig. 1.
b) 512^3 DNS of decaying isotropic turbulence ($\mathrm{Re}_\lambda = 63.5$) that was filtered to both 64^3 and 32^3 synthetic LES fields, see Fig. 2.

In addition, correlations at the tensor level were also obtained when using smooth filters (here applied in wave space) with $G(\boldsymbol{x}/\Delta) = \prod_{i=1,3} G(x_i/\Delta)$, $G(\boldsymbol{k}\,\Delta) = \prod_{i=1,3} G(k_i\,\Delta)$, such as the Gaussian (of same standard deviation as the top-hat),

$$G\left(\frac{x_i}{\Delta}\right) = \left(\frac{6}{\pi}\right)^{1/2}\exp\left(-6\left(\frac{x_i}{\Delta}\right)^2\right)\ ; \quad G\left(k_i\,\Delta\right) = \exp\left(-\frac{1}{6}\left(\frac{k_i\,\Delta}{2}\right)^2\right)\ ,$$

and the top-hat,

$$G\left(\frac{x_i}{\Delta}\right) = 1 \quad \text{if } \left|\frac{x_i}{\Delta}\right| < \frac{1}{2}\,, \quad 0 \quad \text{otherwise}\,; \quad G\left(k_i\,\Delta\right) = \frac{\sin\left(\frac{k_i\,\Delta}{2}\right)}{\left(\frac{k_i\,\Delta}{2}\right)}\ ,$$

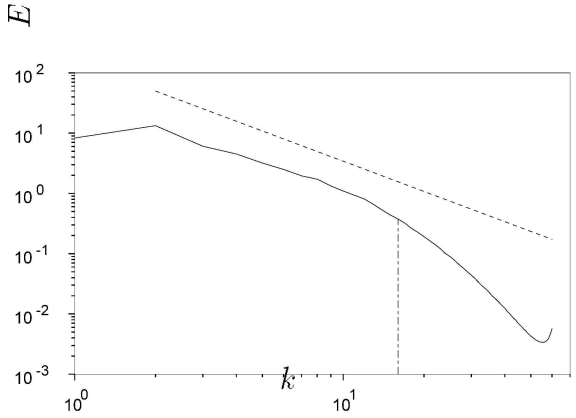

FIGURE 1. Spectrum of the 128^3 DNS ($\mathrm{Re}_\lambda = 95.8$). Also shown is the cut used to produce the 32^3 synthetic LES field. ——— , $E(k)$; ---- , $K^{-5/3}$.

to generate synthetic LES fields from the 128^3 DNS data (i.e., DNS with $k_{\max} = 64$). The cutoff wavenumber was set to $k_{\max} = 16$, hence $\Delta = \pi/k_{\max} = \pi/16$. Notice that, with smooth filters, the synthetic LES field still contains contributions from all original modes.

Many different LES models were investigated:
Model 1 (eddy-viscosity type, tensor modeling):

$$\overline{\tau}_{ij}^{*\,M} = -2\overline{\nu_t\,\overline{S}_{ij}} \qquad \text{with} \qquad \overline{S}_{ij} = \frac{1}{2}\left(\frac{\partial \overline{u}_i}{\partial x_j} + \frac{\partial \overline{u}_j}{\partial x_i}\right) .$$

Different choices for the $1/T$ scaling that appears in the eddy-viscosity were investigated:

$$\nu_t = C\,\Delta^2\,\left(2\,\overline{S}_{ij}\overline{S}_{ij}\right)^{1/2} , \qquad (a)$$

$$\nu_t = C\,\Delta^2\,\left(\overline{\omega}_i\overline{\omega}_i\right)^{1/2} , \qquad (b)$$

$$\nu_t = C\,\Delta^2\,\left(\epsilon/\Delta^2\right)^{1/3} , \qquad (c)$$

$$\nu_t = C\,\Delta^2\,\left(2\,\overline{\omega}_i\overline{S}_{ij}\overline{\omega}_j\right)/\left(\overline{\omega}_i\overline{\omega}_i\right) , \qquad (d)$$

$$\nu_t = C\,\Delta^2\,\left(2\,\overline{\omega}_i\overline{S}_{ij}\overline{\omega}_j\right)^{1/3} , \qquad (e)$$

where ϵ is the rate of energy transfer within the inertial range (assumed constant) and $\overline{\boldsymbol{\omega}} = \nabla \times \overline{\boldsymbol{u}}$ is the large-scale vorticity. The first choice is the classical Smagorinsky's scaling based on local dissipation by the large scales (e.g., see reviews by

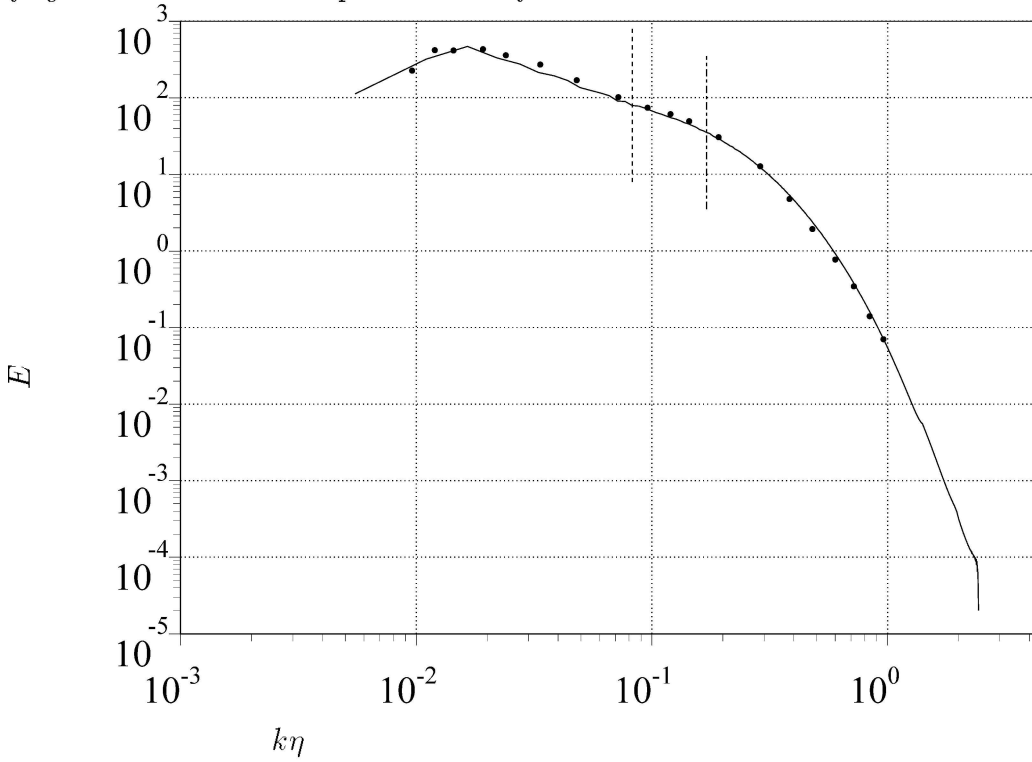

FIGURE 2. Spectrum of the 512^3 DNS ($\mathrm{Re}_\lambda = 63.5$). Also shown are the cuts used to produce the 64^3 and 32^3 synthetic LES fields. • : Comte-Bellot and Corrsin experimental data at $\mathrm{Re}_\lambda = 65.1$. k normalized by Kolmogorov scale η.

Rogallo & Moin 1984, Lesieur *et al.* 1995). Consider the eigenvalues λ_1, λ_2 and λ_3 of the rate-of-strain tensor, with $\lambda_1+\lambda_2+\lambda_3 = S_{kk} = 0$. The scaling then produces an eddy-viscosity proportional to $\left(2\left(\lambda_1^2+\lambda_2^2+\lambda_3^2\right)\right)^{1/2}$.

The second choice is based on local enstrophy of the large scales (e.g., Mansour *et al.* 1978). Recalling the identity

$$2\,S_{ij}S_{ij} = \omega_i\omega_i + 2\,\frac{\partial}{\partial x_i}\frac{\partial}{\partial x_j}\left(u_i u_j\right)\ ,$$

together with the Poisson equation for pressure, it appears that, to first order, the two scalings differ by the local pressure Laplacian (which can have either sign).

The third choice was proposed by Carati *et al.* (1995b) and is referred to as the 'Kolmogorov' scaling. If, following Smagorinsky, local equilibrium between the rate of energy transfer within the inertial range is identified with the subgrid-scale dissipation $\epsilon \approx -\overline{\tau}^{*}_{ij}{}^{M}\,\overline{S}_{ij}$, one recovers the classical Smagorinsky's model for the eddy-viscosity. The Kolmogorov scaling has the practical advantage over the other models that fewer filtering operations are required when implementing the dynamic procedure as in Germano *et al.* (1991), Ghosal *et al.* (1992), Moin & Jiménez (1993), Moin *et al.* (1994), Ghosal *et al.* (1995), Carati *et al.* (1995a). When

developing the dynamic procedure in the present formulation, one obtains

$$-2\,\Delta^{4/3}\left[\left(\frac{\widehat{\Delta}}{\Delta}\right)^{4/3} C'\,\widehat{\overline{S}}_{ij} - \widehat{C'\,\overline{S}_{ij}}\right] = \left(\widehat{\overline{u}_i\,\overline{u}_j} - \widehat{\overline{u}_i}\,\widehat{\overline{u}_j}\right)^* \ .$$

where $\widehat{\psi}$ is an additional 'test filter' of the LES field, at scale $\widehat{\Delta}$, where C' stands for the *dimensional* product $C\,\epsilon^{1/3}$, and where it has been assumed that both filters lie in the inertial range so that ϵ is indeed the same at both filter sizes. Since the dynamic procedure also assumes that the model coefficient C is invariant with filtering scale in that range, it turns out that C' is also invariant with filtering scale and is, in fact, what is determined by the dynamic procedure.

The fourth scaling was proposed by Winckelmans (1995) and is based on the relative rate of change of the large scale enstrophy due to 3-D stretching,

$$\frac{1}{\overline{\omega}_i\overline{\omega}_i}\frac{D}{Dt}\left(\overline{\omega}_i\overline{\omega}_i\right) = 2\,\frac{\overline{\omega}_i\overline{S}_{ij}\overline{\omega}_j}{\overline{\omega}_i\overline{\omega}_i} \ .$$

This scaling selects the eigenvalues used to compute the eddy-viscosity according to the relative orientation between $\overline{\boldsymbol{\omega}}$ and the principal axes (eigenvectors) of the rate-of-strain tensor. Indeed, writing the components of $\overline{\boldsymbol{\omega}}$ in the system of principal axes as $(\overline{\omega}_1, \overline{\omega}_2, \overline{\omega}_3)$, this scaling produces an eddy-viscosity proportional to $2\left(\lambda_1\overline{\omega}_1^2 + \lambda_2\overline{\omega}_2^2 + \lambda_3\overline{\omega}_3^2\right) / \left(\overline{\omega}_1^2 + \overline{\omega}_2^2 + \overline{\omega}_3^2\right)$. Hence a vorticity-weighted average of the eigenvalues is used to produce the eddy-viscosity. This scaling produces a negative eddy viscosity scaling in regions where enstrophy is decreasing. To ensure positivity, one can use either $|d|$ or $d_+ = \max(d, 0)$.

For completeness, a fifth scaling is considered, which is based on the rate of change of enstrophy, hence an eddy viscosity proportional to $\left(2\left(\lambda_1\overline{\omega}_1^2 + \lambda_2\overline{\omega}_2^2 + \lambda_3\overline{\omega}_3^2\right)\right)^{1/3}$.

Models other than the classical LES model (Model 1) were also investigated:
Model 2 (eddy-viscosity type, solenoidal force modeling):

$$\overline{g}^{*\,M} = -\nabla \times \left(\overline{\nu_t\,\overline{\omega}}\right) \ .$$

Model 3 (hyper eddy-viscosity type, tensor modeling):

$$\overline{\tau}_{ij}^{*\,M} = 2\,\Delta^2\,\overline{\nu_t\,\nabla^2\overline{S}_{ij}} \ .$$

Model 1+3 (mixed eddy-viscosity and hyper eddy viscosity type, tensor modeling):

$$\overline{\tau}_{ij}^{*\,M} = -2\left(\overline{\nu_{t1}\,\overline{S}_{ij}} - \Delta^2\,\overline{\nu_{t2}\,\nabla^2\overline{S}_{ij}}\right) \ .$$

Model 1+4 (mixed, simplest non eddy-viscosity type, tensor modeling):

$$\overline{\tau}_{ij}^{*\,M} = -2\left(\overline{\nu_t\,\overline{S}_{ij}} + C_2\,\Delta^2\,\overline{\left(\overline{S}_{il}\,\overline{S}_{lj}\right)^*}\right) \ .$$

We are unaware of any published results describing Model 3 or Model 1+3. However, Cerutti and Meneveau (1996, private communication) have also considered this

model. Model 1+4 is one of the many models investigated by Lund and Novikov (1992) where they considered all possible models with the sgs tensor function only of the strain and rotation rate tensors.

Notice that one can even build models that give a decent (i.e., as good as other models) correlation at the tensor level but give zero solenoidal force, hence zero effect on the dynamics of the filtered velocity field, e.g.,

$$\overline{\tau}_{ij}{}^{M} = C\,\Delta^2\,\frac{\partial}{\partial x_i}\frac{\partial}{\partial x_j}\left(\overline{u}_l\overline{u}_l\right)\ .$$

Such models should, of course, never be used. Nevertheless, they make the point that correlation at the tensor level does not necessarily mean good dynamics. What really matters is the solenoidal forcing.

Finally, scale similarity models of Bardina's type, Models B, were also investigated (e.g., see Horiuti 1993, Zang et al. 1993, Liu et al. 1994, Salvetti & Banerjee 1995). The combinations considered were:

$$C\,\left(\widehat{\overline{u}_i\overline{u}_j} - \widehat{\widehat{\overline{u}}_i\widehat{\overline{u}}_j}\right)\ , \qquad (a)$$

$$C\,\left(\widehat{\overline{u}_i\overline{u}_j} - \widehat{\overline{u}}_i\widehat{\overline{u}}_j\right)\ , \qquad (b)$$

$$C\,\left(\overline{u}_i\overline{u}_j - \widehat{\overline{u}}_i\widehat{\overline{u}}_j\right)\ , \qquad (c)$$

$$C\,\left(\widehat{\widehat{\overline{u}}_i\widehat{\overline{u}}_j} - \widehat{\overline{u}}_i\widehat{\overline{u}}_j\right)\ , \qquad (d)$$

where the additional filtering of the LES field was done at twice the size of the original filter, and with the same filter type. Model Ba is the filtering of $\overline{u}_i\overline{u}_j - \widehat{\overline{u}}_i\widehat{\overline{u}}_j$ and is 'similar' to $\overline{\tau}_{ij}$, which is the original filtering of $u_iu_j - \overline{u}_i\overline{u}_j$. Model Bb is similar to $\tau_{ij} = \overline{u_iu_j} - \overline{u}_i\overline{u}_j$. Model Bc was also investigated, in *a priori* testing, in Meneveau & Lund (1992). Model Bd is the remainder, after second filtering, of $\widehat{\overline{u}}_i\widehat{\overline{u}}_j$, and is thus not expected to perform well.

2. Optimization of the coefficient(s) and correlations

We first consider optimization of the model's coefficient(s) when no spatial variation is allowed. This is a natural requirement as the models are being compared with DNS data in isotropic turbulence. For each level, the value of C that provides the minimum error, in the least square sense, between 'exact' and 'modeled' subgrid-scale quantities is evaluated. Defining

$$\overline{\tau}^*_{ij}{}^{M} = C_\tau\,\overline{m}^*_{ij}\ , \quad \overline{g}^*_i{}^{M} = C_g\,\overline{m}^*_i\ ,$$

and $\langle\cdot\rangle$ as integration over physical space, one then obtains:
At the traceless tensor level:

$$C_\tau = \frac{\langle\overline{\tau}^*_{kl}\,\overline{m}^*_{kl}\rangle}{\langle\overline{m}^*_{kl}\,\overline{m}^*_{kl}\rangle}\ .$$

At the solenoidal force level:

$$C_g = \frac{\langle \overline{g}^*_k \, \overline{m}^*_k \rangle}{\langle \overline{m}^*_k \, \overline{m}^*_k \rangle} \; .$$

At the scalar level (= dissipation level):

$$\overline{d}^* = \overline{u}_k \overline{g}^*_k \; , \qquad \overline{d}^{*M} = \overline{u}_k \overline{g}^{*M}_k = C_d \, \overline{m}^* \; , \qquad C_d = \frac{\langle \overline{d}^* \, \overline{m}^* \rangle}{\langle \overline{m}^* \, \overline{m}^* \rangle} \; .$$

For models with two coefficients, defining

$$\overline{\tau}^{*M}_{ij} = C_{\tau 1} \, \overline{m}^*_{ij} + C_{\tau 2} \, \overline{n}^*_{ij} \; ,$$

the least-square optimization then leads to

$$\begin{pmatrix} \langle \overline{m}^*_{kl} \, \overline{m}^*_{kl} \rangle & \langle \overline{m}^*_{kl} \, \overline{n}^*_{kl} \rangle \\ \langle \overline{m}^*_{kl} \, \overline{n}^*_{kl} \rangle & \langle \overline{n}^*_{kl} \, \overline{n}^*_{kl} \rangle \end{pmatrix} \begin{pmatrix} C_{\tau 1} \\ C_{\tau 2} \end{pmatrix} = \begin{pmatrix} \langle \overline{\tau}^*_{kl} \, \overline{m}^*_{kl} \rangle \\ \langle \overline{\tau}^*_{kl} \, \overline{n}^*_{kl} \rangle \end{pmatrix} \; ,$$

and similarly for the coefficients at the force and dissipation levels.

The correlations between 'exact' and 'modeled' subgrid-scale quantities are defined in the usual way,

$$\eta_\tau = \frac{\langle \overline{\tau}^*_{kl} \, \overline{\tau}^{*M}_{kl} \rangle}{\langle \overline{\tau}^*_{kl} \, \overline{\tau}^*_{kl} \rangle^{1/2} \langle \overline{\tau}^{*M}_{kl} \, \overline{\tau}^{*M}_{kl} \rangle^{1/2}} \; ,$$

$$\eta_g = \frac{\langle \overline{g}^*_k \, \overline{g}^{*M}_k \rangle}{\langle \overline{g}^*_k \, \overline{g}^*_k \rangle^{1/2} \langle \overline{g}^{*M}_k \, \overline{g}^{*M}_k \rangle^{1/2}} \; ,$$

$$\eta_d = \frac{\langle \overline{d}^* \, \overline{d}^{*M} \rangle}{\langle \overline{d}^* \, \overline{d}^* \rangle^{1/2} \langle \overline{d}^{*M} \, \overline{d}^{*M} \rangle^{1/2}} \; .$$

One interesting question is posed when using mixed models instead of the simplest models (e.g., using Model 1+3 instead of Model 1 alone or Model 3 alone): by how much can one expect to improve the correlation? Part of the answer lies in the following identity:

$$\left(\eta^{m+n}_\tau\right)^2 = \frac{(\eta^m_\tau)^2 + (\eta^n_\tau)^2 - 2 \, \eta^m_\tau \, \eta^n_\tau \, \eta^n_m}{1 - (\eta^n_m)^2} \; ,$$

where η^b_a stands for the correlation between a and b. Upper and lower bounds are obtained as:

$$\max\left((\eta^m_\tau)^2 , (\eta^n_\tau)^2\right) \leq \left(\eta^{m+n}_\tau\right)^2 \leq (\eta^m_\tau)^2 + (\eta^n_\tau)^2 \; .$$

The above formulas also hold for correlations at the force or energy dissipation levels by replacing η_τ by η_g or η_d. The best situation occurs when the two terms used

in the models (a) each correlate well with the exact subgrid-scale quantity, and (b) are not highly correlated with each other. This is unfortunately not the case for all models tested in this paper (see results), as well as in other papers (e.g., Lund & Novikov 1992).

We then go on to consider local optimization of the model's coefficient(s) where spatial variation is allowed. Although one usually uses dynamic LES models with coefficient(s) that are averaged (and hence uniform) in the directions of flow homogeneity (here all three directions), the present study is justified by the hope that some model, in some formulation, might exhibit a better behavior than the others in terms of coefficient(s) uniformity. In the same spirit, it is believed that dynamic models will then have to work less hard, e.g., require less averaging of the coefficient(s) obtained dynamically.

The above least square optimization is then carried out locally, at the tensor level. For models with one coefficient, the local optimization leads to

$$C_\tau = \frac{\overline{\tau}^*_{kl}\,\overline{m}^*_{kl}}{\overline{m}^*_{kl}\,\overline{m}^*_{kl}} \ .$$

For models with two coefficients, the linear system is solved locally to determine $C_{\tau 1}$ and $C_{\tau 2}$. The local optimization can be done only at the tensor level. Indeed, the force, being the divergence of the sgs tensor, must remain written in conservative form (so as to have zero global integral in the case of isotropic turbulence). Since C_τ now depends on space, it cannot be pulled out of a derivative such as $\partial\left(C_\tau \overline{m}^*_{ij}\right)/\partial x_j$. (If one were to relax the constraint that the force be conservative, an optimization at the force level would, of course, be possible.)

Correlations are then computed in the same way as above, at all three levels. At the tensor level, they are now artificially much higher than those obtained with uniform C. Since the Cs are optimized locally, their spatial variation is quite high, including regions of negative values. Interesting quantities are evaluated and reported: mean, rms $\left(\langle C^2\rangle - \langle C\rangle^2\right)^{1/2}$, and normalized pdf, the better models exhibiting a sharper (i.e. smaller rms) pdf which is also more skewed towards positive C.

3. Vorticity-velocity formulation and models investigated

Consider LES in the vorticity-velocity formulation:

$$\frac{\partial \overline{\omega}_i}{\partial t} + \frac{\partial}{\partial x_j}\left(\overline{\overline{\omega}_i \overline{u}_j} - \overline{\overline{\omega}_j \overline{u}_i}\right) + \frac{\partial \overline{\gamma}_{ij}}{\partial x_j} = \nu \frac{\partial}{\partial x_j}\frac{\partial \overline{\omega}_i}{\partial x_j} \ ,$$

with the subgrid-scale antisymmetric tensor defined as

$$\gamma_{ij} \stackrel{\text{def}}{=} \left(\overline{\omega_i u_j} - \overline{\omega}_j \overline{u}_i\right) - \left(\overline{\omega}_i \overline{u}_j - \overline{\omega}_j \overline{u}_i\right) = \overline{C}_{ij} + \overline{R}_{ij} + L'_{ij} \ ,$$

$$\overline{\gamma}_{ij} \stackrel{\text{def}}{=} \left(\overline{\omega_i u_j} - \overline{\omega}_j \overline{u}_i\right) - \left(\overline{\overline{\omega}_i \overline{u}_j} - \overline{\overline{\omega}_j \overline{u}_i}\right) = \overline{C}_{ij} + \overline{R}_{ij} \ ,$$

where

$$\overline{C}_{ij} = \left(\overline{\overline{\omega}_i u'_j} - \overline{\overline{\omega}_j u'_i}\right) + \left(\overline{\omega'_i \overline{u}_j} - \overline{\omega'_j \overline{u}_i}\right) \ ,$$

$$\overline{R}_{ij} = \overline{\omega'_i u'_j} - \overline{\omega'_j u'_i} \ ,$$

$$L'_{ij} = \left(\overline{\overline{\omega}_i \overline{u}_j} - \overline{\overline{\omega}_j \overline{u}_i}\right) - \left(\overline{\omega}_i \overline{u}_j - \overline{\omega}_j \overline{u}_i\right) = \left(\overline{\omega}_i \overline{u}_j - \overline{\omega}_j \overline{u}_i\right)' \ .$$

Scaling	C_τ	C_g	C_d	$C_d{}'$	η_τ	η_g	η_d	$\langle C_\tau \rangle$	$\frac{\text{rms}}{\text{mean}}$	η_τ	η_g	η_d
a	0.0086	0.016	0.013	0.0098	0.12	0.29	0.34	0.014	4.4	0.57	0.60	0.59
b	0.012	0.019	0.016	0.013	0.13	0.26	0.32	0.016	4.1	0.56	0.59	0.58
c	0.21*	0.35*	0.29*	0.21*	0.13	0.28	0.33	0.23*	4.0	0.57	0.59	0.59
d	0.013	0.037	0.036	0.041	0.07	0.20	0.27	0.012	15.0	0.57	0.60	0.59
|d|	0.019	0.043	0.036	0.031	0.10	0.26	0.32	0.036	5.8	0.57	0.60	0.59
d_+	0.019	0.037	0.031	0.024	0.11	0.27	0.33	0.032	4.8	0.57	0.60	0.59
e	0.011	0.029	0.028	0.039	0.07	0.20	0.27	0.0082	16.0	0.57	0.59	0.58
|e|	0.017	0.032	0.027	0.028	0.11	0.26	0.31	0.028	5.1	0.56	0.59	0.58
e_+	0.017	0.028	0.022	0.022	0.13	0.27	0.33	0.023	4.2	0.56	0.59	0.58

Table 1. Investigation of the influence of scaling. Model 1, $128^3 \rightarrow 32^3$ with sharp cutoff. ($*$: value of $C\,\epsilon^{1/3}$).

LES in the vorticity-velocity formulation is a natural choice which requires modeling only three quantities. Defining $\overline{\beta}_1 = \overline{\gamma}_{23} = -\overline{\gamma}_{32}$, $\overline{\beta}_2 = \overline{\gamma}_{31} = -\overline{\gamma}_{13}$, $\overline{\beta}_3 = \overline{\gamma}_{12} = -\overline{\gamma}_{21}$, together with $\overline{\gamma}_{11} = \overline{\gamma}_{22} = \overline{\gamma}_{33} = 0$, one obtains $\nabla \cdot \overline{\boldsymbol{\gamma}} = \nabla \times \overline{\boldsymbol{\beta}}$. Hence, modeling is already at the 'vector' level, since modeling $\overline{\boldsymbol{\gamma}}$ is really modeling $\overline{\boldsymbol{\beta}}$. Moreover, it is already in the form of a solenoidal 'forcing', $\nabla \times \overline{\boldsymbol{\beta}}$. For instance, the equivalent of the classical Smagorinsky's model is simply:
Model 1 (eddy-viscosity type):

$$\overline{\gamma}_{ij}{}^M = -2\,\overline{\overline{\nu}_t\,\overline{r}_{ij}} \qquad \text{with} \qquad \overline{r}_{ij} = \frac{1}{2}\left(\frac{\partial \overline{\omega}_i}{\partial x_j} - \frac{\partial \overline{\omega}_j}{\partial x_i}\right) ,$$

which is identical to doing:

$$\frac{\partial \overline{\boldsymbol{\omega}}}{\partial t} + \nabla \cdot (\overline{\overline{\boldsymbol{\omega}}\,\overline{\boldsymbol{u}}} - \overline{\overline{\boldsymbol{u}}\,\overline{\boldsymbol{\omega}}}) = \nabla \times \left(\overline{\overline{\nu}_t\,\nabla^2 \overline{\boldsymbol{u}}}\right) + \nu \nabla^2 \overline{\boldsymbol{\omega}} \; .$$

Another model investigated is:
Model 2 (hyper eddy-viscosity type):

$$-\Delta^2\,\nabla \times \left(\overline{\overline{\nu}_t\,\nabla^4 \overline{\boldsymbol{u}}}\right) \; .$$

4. Results and discussion

The velocity-pressure LES formulation is considered first, with the classical Model 1 but different scalings. The results are compiled in Table 1 for the case $128^3 \rightarrow 32^3$ with sharp cutoff.

For models that can produce local negative scaling, s, it is always better to restrict it to positive values by using $|s|$ or $s_+ = \max(s, 0)$: better correlations are obtained in the case of uniform C, and sharper distribution of C in the case of variable C_τ (smaller ratio 'rms/mean', e.g., 4-6 instead of 15-16). Of the two options, $|s|$ is always slightly better than s_+.

For cases with uniform C (optimized at each level), the correlations are different at each level, typically $\eta_\tau \approx 0.12$, $\eta_g \approx 0.27$, and $\eta_d \approx 0.33$. The choice for the $1/T$

scaling is found to be unimportant as it does not affect the correlations significantly. Since the model represents only a crude estimate of the sgs stresses, the correlations obtained at the tensor level are quite low. Things improve a bit when considering correlation at the force level, and even more so at the dissipation level. This is to be expected as one has to work less hard in the modeling effort: 5 degrees of freedom versus 3 versus 1. Results in Lund & Novikov (1992) and Clark *et al.* (1979) for isotropic turbulence report $\eta_\tau \approx 0.2$ (such correlations are also obtained here, as presented at the end of this section), Piomelli *et al.* (1988) for turbulent channel flow, and McMillan & Ferziger (1979) for homogeneous shear flow reporting $\eta_\tau \approx 0.1$. In the case of uniform C, the correlations only measure the 'alignment' between the model and the exact quantities, not the magnitude. Indeed, C drops out of the three equations defining the correlations. In particular, one could use a value which is such that the global dissipation obtained with the model, $\langle \overline{d}^{*M} \rangle$, be equal to the exact global dissipation, $\langle \overline{d}^{*} \rangle$: $C_d{}' = \langle \overline{d}^{*} \rangle / \langle \overline{m}^{*} \rangle$. These values are also reported in the tables.

For cases with variable C_τ (optimized locally at the tensor level), the correlations are pretty much the same at all levels. To attain correlations in the range 0.56-0.60, the model has to 'work hard': highly varying C_τ field as seen in the ratio rms/mean 4-5 and in the normalized pdf of Fig. 3.

An investigation is also carried out to evaluate the relative participation of the two terms $\overline{C}^*_{ij}$ and $\overline{R}^*_{ij}$ in in the correlations, see Table 2. As expected from the mathematical definitions of these terms, the model correlates better with $\overline{C}^*_{ij}$ than with $\overline{R}^*_{ij}$. It also correlates better with $\overline{C}^*_{ij} + \overline{R}^*_{ij}$ than with $\overline{C}^*_{ij}$ alone.

$\overline{C}^*_{ij}$	$\overline{R}^*_{ij}$	η_τ	η_g	η_d
no	yes	0.060	0.102	0.174
yes	no	0.108	0.278	0.317
yes	yes	0.116	0.286	0.339

Table 2. Contributions of $\overline{C}^*_{ij}$ and $\overline{R}^*_{ij}$ to the correlations; Model 1 with scaling (a); $128^3 \rightarrow 32^3$ with sharp cutoff.

Model 2 is considered next. This model is not obtained by taking the curl of Model 1 (it would if ν_t were uniform). Nevertheless, since the choice of scaling was found to be unimportant with Model 1, which means that very local variation of ν_t are unimportant, Model 2 is expected to perform as Model 1. This is indeed found to be the case. For scaling (a): $C_g = 0.020$, $C_d = 0.016$, $\eta_g = 0.29$, $\eta_d = 0.34$.

Model 3 is considered next. The results are reported in Table 3 and in Fig. 3. This model performs significantly better than Model 1 at all three levels, and for both cases of uniform and variable coefficient. In particular, with variable C_τ, the pdf is sharper (ratio rms/mean of 3.3 instead of 4.4) and more skewed to the right.

Model 1+3 with uniform coefficients does not perform substantially better than Model 3 alone ($\eta_g = 0.344$ instead of 0.334). This is due to the fact that $\overline{S}_{ij}$

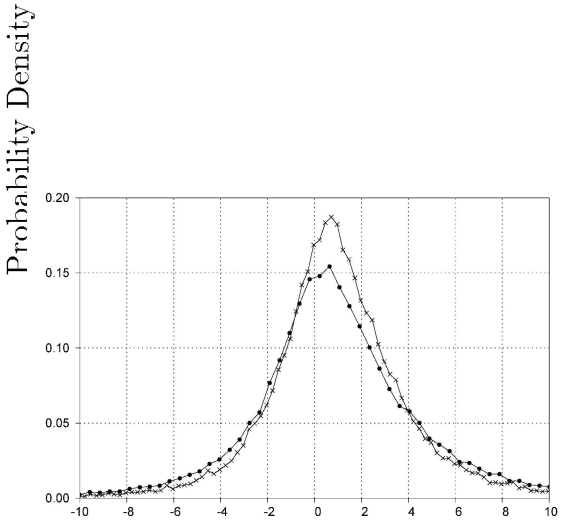

FIGURE 3. Normalized pdf for Model 1 (•) and Model 3 (×) with scaling (a); $128^3 \rightarrow 32^3$ with sharp cutoff.

Model	C_τ	C_g	C_d	η_τ	η_g	η_d	$\langle C_\tau \rangle$	$\frac{\text{rms}}{\text{mean}}$	η_τ	η_g	η_d
1	0.0086	0.016	0.013	0.12	0.29	0.34	0.014	4.4	0.57	0.60	0.59
3	0.0030	0.0037	0.0034	0.16	0.33	0.39	0.0040	3.3	0.59	0.62	0.63
1+3	-0.0077	-0.014	-0.012	0.17	0.34	0.40	-0.0059	24	0.75	0.76	0.76
	0.0046	0.0062	0.0060				0.0053	5.6			
4	0.0089	-0.073	-0.076	0.031	-0.21	-0.29	0.019	12	0.57	0.54	0.53
1+4	0.014	0.015	0.012	0.16	0.29	0.34	0.019	4.6	0.75	0.74	0.73
	0.039	-0.011	-0.012				0.047	6.9			

Table 3. Comparison of Model 3 and Model 1+3, Model 4 and Model 1+4, with Model 1; scaling (a); $128^3 \rightarrow 32^3$ with sharp cutoff.

and $\nabla^2 \overline{S}_{ij}$ are highly correlated to each other (relative correlations $\eta_\tau = 0.87$, $\eta_g = 0.94$, $\eta_d = 0.95$). It is found that this model corresponds to diffusion with the hyperviscosity term ($C_2 > 0$) corrected by some antidiffusion with the viscosity term ($C_1 < 0$). In the case with variable coefficients, it is found that $C_{\tau 1}$ must vary a lot in order to bring the correlations to 0.75–0.76: very high ratio of rms/mean for $C_{\tau 1}$.

Finally, Model 1+4 is investigated. Model 4 alone performs very poorly: in the case of uniform coefficient, the optimization leads to a coefficient of different sign whether the correlation is formed at the tensor level, or at the force and dissipation levels; in the case with variable coefficient, a ratio rms/mean of 12 is obtained.

Model 1+4 with uniform coefficients does not perform better than Model 1 alone. This is in accordance with results in Lund & Novikov (1992). This is due not only to the high correlations between the two terms (relative correlations $\eta_\tau = -0.55$, $\eta_g = -0.67$, $\eta_d = -0.82$), but also to the low correlations of Model 4 alone. In that respect, Model 1+3 performs significantly better than Model 1+4. In the case with variable coefficients, the correlations for Model 1+4 are in the 0.73-0.75 level, with not much of an increase in the ratio rms/mean for $C_{\tau 1}$, and even a decrease in the ratio for $C_{\tau 2}$. This is in contrast with what was obtained with Model 1+3.

The case where smooth filters are applied to the DNS data is also investigated. In that case, correlations are obtained at the tensor level only. The reason being that the filtered data for the τ_{ij} was computed on the original 128^3 grid, but was only sampled, for output, on a 32^3 subset of that grid. Since it still contains very significant contributions from all original modes, this data cannot be properly differentiated to obtain the forces. All possible contributions to the sgs tensor were considered and were correlated with Model 1, see Table 4.

$L_{ij}^{*\prime}$	$\overline{C}_{ij}^{*}$	$\overline{R}_{ij}^{*}$	C_τ	η_τ	$\langle C_\tau \rangle$	$\frac{\text{rms}}{\text{mean}}$	η_τ
no	no	yes	0.00062	0.083	0.0014	7.2	0.41
no	yes	no	0.0054	0.080	0.011	12	0.42
no	yes	yes	0.0060	0.084	0.012	11	0.42
yes	no	no	0.0047	0.067	-0.0027	47	0.41
yes	no	yes	0.0053	0.077	-0.0014	92	0.41
yes	yes	no	0.010	0.27	0.0083	2.8	0.34
yes	yes	yes	0.011	0.26	0.0097	2.6	0.33

Table 4. Gaussian filtering of the 128^3 DNS; Model 1 with scaling (a).

We feel that the cutoff filter is the most appropriate for generating synthetic LES fields from DNS data as it completely eliminates the 'small scale' information that will never be present in a large eddy simulation. In that sense, *a priori* tests using smooth filters such as the Gaussian are of a more academic interest. Indeed, an LES simulation would not be able to capture with the 32^3 grid the 'small scale' information which is still present after smooth filtering of the 128^3 DNS data. With the Gaussian, the filter value at the cutoff wavenumber (i.e., at the edge of the 32^3 grid) is $0.663^3 = 0.291$, which is still very significant. At twice that wavenumber, it has dropped to $0.193^3 = 0.0072$. It thus can be argued that a 64^3 grid (or so) would be needed to correctly capture the important part of the fine grain information left after Gaussian filtering.

Proceeding nevertheless with this study, one finds that the case where Model 1 is correlated with $\overline{C}_{ij}^{*} + \overline{R}_{ij}^{*} + L_{ij}^{*\prime}$ $(= \tau_{ij}^{*})$ performs quite well: $\eta_\tau = 0.26$ for the case with uniform coefficient, rms/mean of only 2.6 to reach $\eta_\tau = 0.33$ for the case with variable coefficient. Similarly for the case $\overline{C}_{ij}^{*} + L_{ij}^{*\prime}$. The cases $L_{ij}^{*\prime}$ and $\overline{R}_{ij}^{*} + L_{ij}^{*\prime}$ perform very poorly: very low correlation in the case with uniform coefficient, extremely high value of rms/mean in the case with variable coefficient.

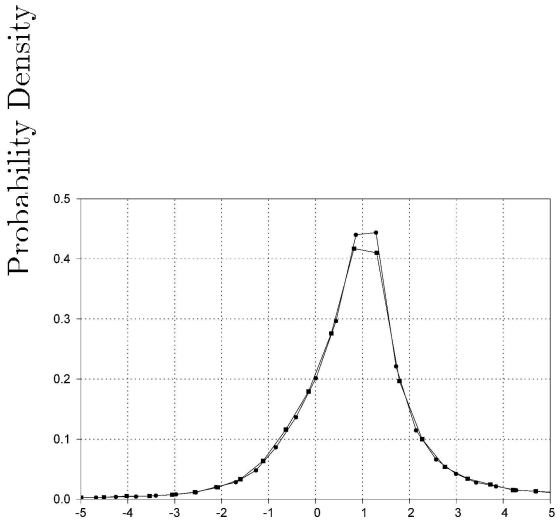

FIGURE 4. Normalized pdf for Model 1 with scaling (a); Gaussian (•) and top-hat (■) filtering of the 128^3 DNS.

All other case are such that $L_{ij}^{*\prime}$ is not included and perform very poorly, e.g., the case $\overline{C}_{ij}^{*} + \overline{R}_{ij}^{*}$ $(= \overline{\tau}_{ij}^{*})$, which has only $\eta_\tau = 0.084$. In conclusion, the correlation with τ_{ij}^{*} is significantly higher than what was obtained with sharp cutoff ($\eta_\tau = 0.26$ instead of 0.12) but the correlation with $\overline{\tau}_{ij}^{*}$ is significantly lower ($\eta_\tau = 0.084$ instead of 0.12). Finally, very similar results are obtained when using the top-hat filter instead of the Gaussian, see e.g., Fig. 4 for very similar pdf's.

The scale similarity models, Models B, are considered next, first with sharp cutoff filter, then with Gaussian filter.

Type	C_τ	C_g	C_d	$C_d{}'$	η_τ	η_g	η_d
a	0.028	0.022	0.084	0.68	0.043	0.017	0.070
b	0.015	0.031	0.083	0.43	0.039	0.034	0.098
c	-0.0054	-0.044	-0.053	1.20	-0.022	-0.12	-0.14
d	0.0076	0.039	0.090	1.2	0.015	0.031	0.075

Table 5. Scale similarity models, $128^3 \rightarrow 32^3$ with sharp cutoff.

With sharp cutoff, Models B are only compared to $\overline{\tau}_{ij}^{*}$ (since $L_{ij}^{*\prime}$ cannot be captured on the 32^3 grid), see Table 5. It is seen that very low levels of correlations are obtained regardless of the Model's type. This is in accordance with results by Meneveau & Lund (1992). Again, one must recall that, in the case of uniform C,

the correlation is independent of C. Nevertheless, when C is optimized as usual, one obtains a very large difference between $C_d{}'$ and C_τ, C_g, C_d, which is also indicative of very poor models. Thus, with sharp cutoff filter, Bardina's type models show essentially no correlation with the relevant sgs quantities: trace-free tensor $\overline{\tau}^*_{ij}$, solenoidal force $\overline{g}^*_i$. In fact, if anything, Models Ba and Bb only correlate a little when the trace of $\overline{\tau}_{ij}$ is kept ($\eta_\tau = 0.13$ and 0.11 respectively).

Type	sgs	C_τ	η_τ	$\langle C_\tau \rangle$	$\frac{\text{rms}}{\text{mean}}$	η_τ
a	τ^*_{ij}	0.14	0.29	0.21	1.8	0.61
	$\overline{\tau}^*_{ij}$	0.57	0.70	0.51	0.93	0.73
b	τ^*_{ij}	0.47	0.70	0.38	0.90	0.74
	$\overline{\tau}^*_{ij}$	0.29	0.25	0.33	2.8	0.53
c	τ^*_{ij}	0.014	0.062	0.0073	48	0.47
	$\overline{\tau}^*_{ij}$	0.37	0.92	0.36	0.57	0.78
d	τ^*_{ij}	0.095	0.20	0.15	2.8	0.57
	$\overline{\tau}^*_{ij}$	-0.47	-0.55	-0.40	1.44	0.64

Table 6. Scale similarity models; Gaussian filtering applied to the 128^3 DNS.

With Gaussian smoothing, things are completely different, see Table 6. Models B are here compared to both τ^*_{ij} and $\overline{\tau}^*_{ij}$. Model Ba is 'similar' to $\overline{\tau}^*_{ij}$ and correlates indeed very well with it: $\eta_\tau = 0.70$ for the case with uniform C, very low rms/mean of 0.93 for the case with variable C. Model Bb is 'similar' to τ^*_{ij} and correlates indeed very well with it: $\eta_\tau = 0.70$ for the case with uniform C, rms/mean of 0.90 for the case with variable C. Model Bc correlates very poorly with τ^*_{ij}, but extremely well with $\overline{\tau}^*_{ij}$: $\eta_\tau = 0.92$ for the case with uniform C, rms/mean of 0.57 for the case with variable C. This is the highest correlation encountered in the course of this study. It is consistent with the 0.8 correlation reported in Meneveau & Lund (1992). Model Bd does not perform well, as expected, since it is the remainder of some quantity after second filtering.

These impressive results are misleading. Indeed, Gaussian filtering of the DNS data produces a synthetic LES field that still contains considerable contributions from the small scales. As this small scale information will not be present in an real LES, results obtained with the sharp cutoff filter are more representative of what might be expected from using Bardina's models in LES.

The vorticity-velocity LES formulation is now considered. The correlation at the antisymmetric tensor level, γ_{ij}, is denoted as C_γ, at the 'forcing' level as C_g, at the 'enstrophy dissipation' level as C_d. The results obtained with the eddy-viscosity model, Model 1, and with the hyper eddy-viscosity model, Model 2, are presented in Table 7.

The eddy-viscosity model in the vorticity-velocity formulation produces significantly higher correlations than its counterpart in the velocity-pressure formulation: in the case of uniform coefficient, $\eta_\gamma = 0.19$ instead of $\eta_\tau = 0.12$, $\eta_g = 0.32$ instead of 0.29, $\eta_d = 0.46$ instead of 0.34; in the case of variable coefficient, $\eta_\gamma = 0.71$

Model	C_γ	C_g	C_d	$C_d{}'$	η_γ	η_g	η_d	$\langle C_\gamma \rangle$	$\frac{\text{rms}}{\text{mean}}$	η_γ	η_g	η_d
1	0.019	0.026	0.019	0.021	0.19	0.32	0.46	0.023	4.6	0.71	0.74	0.80
2	0.0041	0.0046	0.036	0.039	0.23	0.35	0.48	0.0045	4.0	0.73	0.75	0.79

Table 7. Vorticity-velocity formulation; Model 1 and Model 2 with scaling (a); $128^8 \rightarrow 32^3$ with sharp cutoff.

instead of $\eta_\tau = 0.57$, $\eta_g = 0.74$ instead of 0.60, $\eta_d = 0.80$ instead of 0.59, with essentially the same ratio rms/mean as before, and a pdf which is more skewed towards positive C, see Fig. 5.

Again, the hyper eddy-viscosity version of the model performs even better than the eddy-viscosity version, see Table 7 and pdf of Fig. 5.

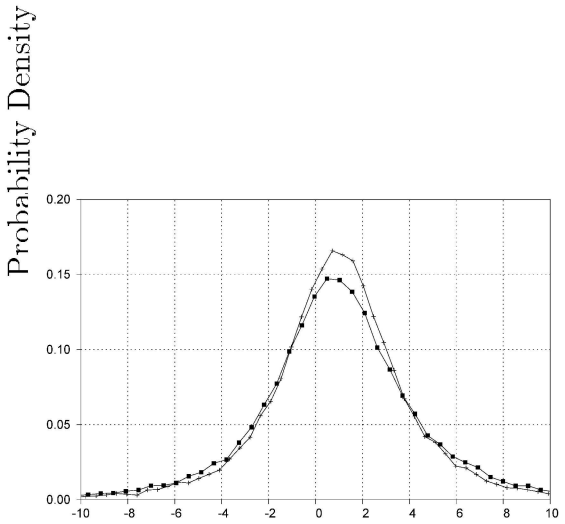

FIGURE 5. Normalized pdf for Model 1 (■) and Model 2 (+) with scaling (a) in the vorticity-velocity formulation; $128^3 \rightarrow 32^3$ with sharp cutoff.

Moreover, one finds for both models that the coefficients optimized globally are close to each other, and that they are also close to the average of the coefficient optimized locally. This is also indicative of good candidate models for LES.

For completeness, the case of smooth filtering of the DNS data is also investigated, see Table 8. The Gaussian and top-hat filter produce similar results. The eddy-viscosity model in the vorticity-velocity formulation performs slightly better than in the velocity-pressure formulation: in the case of uniform coefficient, $\eta_\gamma = 0.28$ instead of 0.26; in the case of variable coefficient, $\eta_\gamma = 0.55$ instead of 0.33, with

Type	sgs	C_γ	η_γ	$\langle C_\gamma \rangle$	$\frac{\text{rms}}{\text{mean}}$	η_γ
Gaussian	γ_{ij}	0.014	0.28	0.014	2.1	0.55
top-hat	γ_{ij}	0.015	0.24	0.016	2.3	0.53
Gaussian	$\overline{\gamma}_{ij}$	0.042	0.051	0.0009	140	0.52
tophat	$\overline{\gamma}_{ij}$	0.050	0.057	0.0029	42	0.53

Table 8. Vorticity-velocity formulation; Gaussian and top-hat filtering of the 128^3 DNS; Model 1 with scaling (a).

a smaller ratio rms/mean (2.1 instead of 2.6). Again, when the L'_{ij} term is not included (i.e., when using $\overline{\gamma}_{ij}$ instead of γ_{ij}), the model correlates very poorly.

So far, all correlations have been obtained using the same 128^3 DNS database in forced isotropic turbulence ($Re_\lambda = 95.8$). With sharp cutoff filter, the filtering was always done from 128^3 DNS to a 32^3 synthetic LES field. An investigation is now done (a) using the same database, but filtering to a 16^3 synthetic LES field, and (b) filtering the 512^3 DNS database in decaying isotropic turbulence ($Re_\lambda = 63.5$) to both 64^3 and 32^3 synthetic LES fields. The regions of the spectra where the cut is done are marked in Figs. 1 and 2. Although there is no pure $k^{-5/3}$ 'inertial range' in this 512^3 computation at such Re_λ, there is 'almost' an inertial range, the 64^3 cut being to the far right of it, and the 32^3 cut being within it. With the 128^3 database, the 32^3 cut is also to the far right of the 'inertial range' (actually probably more at the beginning of the 'dissipation range'), and the 16^3 cut is within the inertial range. Results of this investigation done in the velocity-pressure formulation are reported in Table 9 and in Fig. 6. The results corresponding to the vorticity-velocity formulation are presented in Table 10.

Data	C_τ	C_g	C_d	$C_d{}'$	η_τ	η_g	η_d	$\langle C_\tau \rangle$	$\frac{\text{rms}}{\text{mean}}$	η_τ	η_g	η_d
$128^3 \to 32^3$	0.0086	0.016	0.013	0.0098	0.12	0.29	0.34	0.014	4.4	0.57	0.60	0.59
$128^3 \to 16^3$	0.061	0.077	0.070	0.069	0.18	0.32	0.46	0.11	3.5	0.49	0.38	0.38
$512^3 \to 64^3$	0.016	0.019	0.018	0.018	0.18	0.30	0.42	0.022	3.1	0.59	0.60	0.64
$512^3 \to 32^3$	0.029	0.028	0.028	0.031	0.29	0.39	0.59	0.036	2.0	0.61	0.64	0.73

Table 9. Investigation of different databases and of different cut locations in each database; velocity-pressure formulation; Model 1 with scaling (a); sharp cutoff.

We concentrate on correlations obtained with uniform coefficients. When considering different cuts within the same database, one finds that the cut within the inertial range produces higher correlations than the cut to the far right of that range. We don't see any obvious reason at this time why this should be the case. Nevertheless, this finding holds for both databases investigated and for both formulations.

Notice that the superior performance of the vorticity-velocity formulation over the velocity-pressure formulation is not as marked in the 512^3 runs as it is in the

Data	C_γ	C_g	C_d	$C_d{}'$	η_γ	η_g	η_d	$\langle C_\gamma \rangle$	$\frac{\text{rms}}{\text{mean}}$	η_γ	η_g	η_d
$128^3 \rightarrow 32^3$	0.019	0.026	0.019	0.021	0.19	0.32	0.46	0.023	4.6	0.71	0.74	0.80
$512^3 \rightarrow 64^3$	0.022	0.025	0.023	0.024	0.21	0.29	0.50	0.025	4.3	0.71	0.73	0.81
$512^3 \rightarrow 32^3$	0.032	0.033	0.033	0.035	0.28	0.35	0.62	0.037	3.0	0.73	0.74	0.84

Table 10. Investigation of different databases and of different cut locations in each database; vorticity-velocity formulation; Model 1 with scaling (a); sharp cutoff.

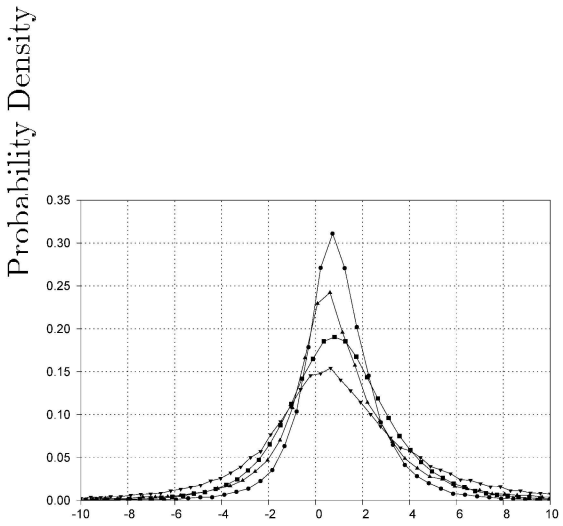

FIGURE 6. Normalized pdf for Model 1 with scaling (a) in the velocity-pressure formulation; $128^3 \rightarrow 32^3$ (∇), $128^3 \rightarrow 16^3$ ($\blacktriangle$), $512^3 \rightarrow 64^3$ ($\blacksquare$), $512^3 \rightarrow 32^3$ ($\bullet$) with sharp cutoff.

128^3 runs. In particular, the $512^3 \rightarrow 32^3$ cases are very comparable when C is uniform (still slightly better when C is allowed to vary).

5. Conclusions

A few conclusions can be made from the investigations done using the sharp cutoff filter to produce the synthetic LES fields from the DNS databases. The choice for the $1/T$ scaling in the eddy-viscosity is found to be unimportant as it does not significantly affect the correlations between modeled and exact sgs quantities at any of the three levels: trace-free tensor, solenoidal forcing, dissipation. It is found that the hyper eddy-viscosity model yields higher correlations than the eddy-viscosity model in both the velocity-pressure and the vorticity-velocity formulations. It thus appears as a good candidate for real LES and should be tested numerically. Scale similarity models exhibit essentially no correlation with the exact sgs quantities

when the sharp cutoff filter is used. The correlations obtained with simple LES models in the vorticity-velocity formulation are higher than those obtained with the counterpart models in the velocity-pressure formulation. This suggests that the vorticity-velocity formulation might be a good candidate for real LES, with reduced sgs modeling error. It certainly appears as a natural choice. It should also be tested numerically in real LES.

Some conclusions are also reached from the investigations done using the Gaussian and top-hat filters in order to produce the synthetic LES fields. It is found that the L'_{ij} contribution is essential in order to produce significant correlations. The correlations are then artificially higher than those obtained with sharp cutoff. Indeed, the filtered field still contains significant small-scale information that would not be available in a real LES. In particular, some scale similarity models exhibit remarkably high correlations when smooth filters are used.

Finally, it is found that the level of obtained correlation is quite sensitive to the database investigated, and to the location of the spectral 'cut' used to produce the synthetic LES field. If anything, our investigation shows that one must exercise caution when comparing correlations reported by different authors and when working with different databases and with different models or formulations.

REFERENCES

Carati, D., Ghosal, S. & Moin, P. 1995 On the representation of backscatter in dynamic localization models. *Phys. Fluids.* **7(3),** 606-16.

Carati, D., Jansen, K. & Lund, T. 1995 A family of dynamic models for large-eddy simulation. *Ann. Res. Briefs*, Center for Turbulence Research (Stanford University/NASA Ames), 35-40.

Cerutti, S. & Meneveau, C. 1996 Statistical equilibrium in 3-D turbulence: implications for hyperviscous and nonlocal subgrid models. *In preparation for journal submission.*

Clark, R. A., Ferziger, J.-H. & Reynolds, W. C. 1979 Evaluation of subgrid-scale models using an accurately simulated turbulent flow. *J. Fluid Mech.* **91,** 1.

Comte-Bellot, G. & Corrsin, S. 1971 Simple Eulerian time-correlation full and narrow-band velocity signals in grid-generated 'isotropic' turbulence. *J. Fluid Mech.* **48,** 273-337.

Germano, M., Piomelli, U., Moin, P. & Cabot, W. 1991 A dynamic subgrid-scale eddy-viscosity model. *Phys. Fluids A.* **3(7),** 1760-65.

Ghosal, S., Lund, T. S. & Moin, P. 1992 A local dynamic model for large-eddy simulation. *Ann. Res. Briefs*, Center for Turbulence Research (Stanford University and NASA Ames), 3-25.

Ghosal, S., Lund, T. S., Moin, P. & Akselvoll, K. 1995 A dynamic localization model for large-eddy simulation of turbulent flows. *J. Fluid Mech.* **286,** 229-255.

HORIUTI, K. 1993 A proper velocity scale for modeling subgrid-scale eddy viscosities in large eddy simulation. *Phys. Fluids A.* **5(1),** 146-57.

LESIEUR, M., COMTE, P. & MÉTAIS, O. 1995 Numerical simulations of coherent vortices in turbulence. *Appl. Mech. Rev.* **48(3),** 121-149.

LIU, S., MENEVEAU, C. & KATZ, J. 1994 On the properties of similarity subgrid-scale models as deduced from measurements in a turbulent jet. *J. Fluid Mech.* **275,** 83-119.

LUND, T. S. & NOVIKOV, E. A. 1992 Parameterization of subgrid-scale stress by the velocity gradient tensor. *Ann. Res. Briefs*, Center for Turbulence Research (Stanford University/NASA Ames), 27-43.

MCMILLAN, O. J. & FERZIGER, J. H. 1979 Direct testing of subgrid-scale models. *AIAA J.* **17,** 1340.

MENEVEAU, C. & LUND, T. S. 1992 Search for subgrid-scale parameterization by projection pursuit regression. *Proceedings of the 1992 Summer Program* Center for Turbulence Research (Stanford University/NASA Ames), 61-82.

MANSOUR, N. N., FERZIGER, J. H. & REYNOLDS, W. C. 1978 *Large-eddy simulation of a turbulent mixing layer.* Report TF-11, Thermosciences Div., Dept. of Mech. Eng., Stanford University.

MOIN, P. & JIMÉNEZ, J. 1993 Large eddy simulation of complex turbulent flows. *AIAA 24th Fluid Dynamics Conference*, Orlando, Fl., AIAA paper 93-3099.

MOIN, P., CARATI, D., LUND, T., GHOSAL, S, & AKSELVOLL, K. 1994 Developments and applications of dynamic models for large eddy simulation of complex flows. *74th Fluid Dynamics Symposium on Application of Direct and Large Eddy Simulation to Transition and Turbulence*, Chania, Crete, Greece, AGARD-CP-551, 1:1-9.

PIOMELLI, U., MOIN, P. & FERZIGER, J. H. 1988 Model consistency in large eddy simulation of turbulent channel flows. *Phys. Fluids.* **31(7),** 1884-91.

ROGALLO R. S. & MOIN, P. 1984 Numerical simulation of turbulent flows. *Ann. Rev. Fluid Mech.* **16,** 99-137.

SALVETTI, M. V. & BANERJEE, S. 1995 A priori tests of a new dynamic subgrid-scale model for finite-difference large-eddy simulations. *Phys. Fluids.* **7(11),** 2831-47.

WINCKELMANS, G. S. 1995 Some progress in large-eddy simulation using the 3-D vortex particle method. *Ann. Res. Briefs*, Center for Turbulence Research (Stanford University/NASA Ames), 391-415.

ZANG, Y., STREET, R. L. & KOSEFF, J. R. 1993 A dynamic mixed subgrid-scale model and its application to turbulent recirculating flows. *Phys. Fluids A.* **5(12),** 3186-96.